Discontinuous Euler instability in nanoelectromechanical systems

Guillaume Weick,[1] Fabio Pistolesi,[2,3] Eros Mariani,[1] and Felix von Oppen[1]

[1] *Dahlem Center for Complex Quantum Systems and Fachbereich Physik, Freie Universität Berlin, D-14195 Berlin, Germany*
[2] *LPMMC, CNRS and Université Joseph Fourier, F-38042 Grenoble, France*
[3] *CPMOH, CNRS and Université de Bordeaux I, F-33405 Talence, France*

(Dated: August 31, 2009)

When a compressive force applied to a rod exceeds a critical value, the rod buckles into a new, symmetry-breaking equilibrium state. Here, we study this Euler buckling instability in nanoelectromechanical systems. We find that the current flow renormalizes the critical force and induces a discontinuous buckling instability in close analogy with tricritical points in the Landau theory of phase transitions. Conversely, the instability also leads to a current blockade at low biases which can be mechanically tuned, providing a controllable switching device at the nanoscale.

Introduction.—The buckling of an elastic rod by a longitudinal compression force F applied to its two ends constitutes the paradigm of a mechanical instability, called buckling instability [1]. It was first studied by Euler in 1744 while investigating the maximal load that a column can sustain [2]. As long as F stays below a critical force F_c, the rod remains straight, while for $F > F_c$ it buckles, as sketched in Fig. 1. The transition between the two states is continuous and the frequency of the fundamental bending mode vanishes at the instability.

There has been much recent interest in exploring buckling instabilities in nanomechanical systems. In the quest to understand the remarkable mechanical properties of nanotubes [3, 4, 5], there have been observations of compressive buckling instabilities in this system [6]. The Euler buckling instability has been observed in SiO_2 nanobeams and shown to obey continuum elasticity theory [7]. There are also close relations with the recently observed wrinkling [8] and possibly with the rippling [9] of suspended graphene samples. Theoretical works have studied the quantum properties of nanobeams near the Euler instability [10, 11, 12, 13], proposing this system to explore zero-point fluctuations of a mechanical mode [11] or to serve as a mechanical qubit [13]. In this work, we consider the Euler buckling instability in a nano-*electro*mechanical system [14]. We find that the interplay of electronic transport and the mechanical instability causes significant qualitative changes both in the nature of the buckling and in the transport properties.

The continuity of the instability and the consequent vanishing of the vibronic frequency at the transition ("critical slowing down") are the key ingredients which allow for an essentially exact solution of the problem. In fact, the vanishing of the frequency implies that the mechanical motion becomes slow compared to the electronic dynamics and an appropriate non-equilibrium Born-Oppenheimer (NEBO) approximation becomes asymptotically exact near the transition. In leading order, the NEBO approximation yields a current-induced conservative force acting on the vibronic mode. At this order, our principal conclusion is that the coupling to the electronic

FIG. 1: (color online) Sketch of a nanobeam (a) in the flat state and (b) the buckled state with two equivalent metastable positions of the rod (solid and dashed lines).

dynamics can change the nature of the buckling instability from a continuous to a discontinuous transition which is closely analogous to tricritical behavior in the Landau theory of phase transitions. Including in addition the fluctuations of the current-induced force as well as the corresponding dissipation leads to Langevin dynamics of the vibrational mode which becomes important in the vicinity of the discontinuous transition. Employing the same NEBO limit to deduce the electronic current, we find that the buckling instability induces a current blockade over a wide range of parameters. This is a manifestation of the Franck-Condon blockade [15, 16, 17] whenever the buckling instability remains continuous but is caused by a novel tricritical blockade when the instability is discontinuous. The emergence of a current blockade in the buckled state suggests that our setup could serve as a mechanically-controlled switching device.

Model.—We consider a vibrating metallic nanobeam connected to source and drain electrodes. The Hamiltonian $H = H_{\rm vib} + H_e + H_c$ modelling our device is composed of three parts: $H_{\rm vib}$ describes the vibrations of the mechanical beam, H_e the electronic degrees of freedom, and H_c the electron-vibron coupling.

Close to the Euler instability, the frequency of the fundamental bending mode of the beam approaches zero, while all higher modes have a finite frequency [1]. This allows us to retain only the fundamental mode of amplitude X and following previous studies [10, 11, 12], we reduce the vibrational Hamiltonian to the form [18]

$$H_{\rm vib} = \frac{P^2}{2m} + \frac{m\omega^2}{2}X^2 + \frac{\alpha}{4}X^4, \qquad (1)$$

which is closely analogous to the Landau theory of contin-

uous phase transitions. In Eq. (1), P is the momentum conjugate to X and the effective mass associated with the fundamental bending mode (for clamped boundary conditions) is $m \simeq 3\sigma L/8$ where σ and L are the linear mass density and the length of the nanobeam, respectively. The vibrational frequency in Eq. (1) reads $\omega^2 = (\kappa_{\rm eff}/\sigma)(2\pi/L)^4(1 - F/F_c)$. It vanishes when F reaches the critical force $F_c = \kappa_{\rm eff}(2\pi/L)^2$, with $\kappa_{\rm eff}$ the effective bending rigidity. The strength of the quartic term reads $\alpha = (\pi/2L)^4 F_c L$. For $F < F_c$ ($\omega^2 > 0$), the beam remains straight as $X = 0$ is the only stable minimum. For $F > F_c$ ($\omega^2 < 0$), the beam buckles into one of the two minima at $\pm X_+ = \pm\sqrt{-m\omega^2/\alpha}$.

The electronic Hamiltonian $H_e = H_d + H_l + H_t + H_{\rm ch}$ describes the Coulomb-blockade physics of the single-electron transistor setup [19], where H_d accounts for the single-particle levels of the metallic dot, H_l for the non-interacting electrons in the leads, H_t for the electronic tunneling between lead and dot, and $H_{\rm ch} = (\hat{n} - C_g V_g)^2/2C_\Sigma$ for the intradot Coulomb repulsion. Here, $C_\Sigma = 2C + C_g$ denotes the total capacitance and $\hat{n}$ the number operator of excess electrons on the dot. (We adopt units in which the electron charge is set equal to unity.) We assume the left and right junctions to have equal capacitances C and tunneling resistances R. The bias voltage V is applied symmetrically between source and drain, and a gate electrode (with capacitance C_g) can tune the dot energy levels via the gate voltage V_g. Coulomb-blockade physics requires that $R \ll h/e^2$. In the absence of the electron-vibron coupling, the electronic dynamics can then be described by rate equations [19]. Focusing on a Coulomb diamond between dot states with N and $N + 1$ electrons and assuming a positive bias voltage much larger than temperature, the two relevant tunneling rates Γ_+ and Γ_- for charging and discharging the dot with an additional electron are given by $\Gamma_\pm = R^{-1}(V/2 \pm \bar{V}_g)\Theta(V/2 \pm \bar{V}_g)$, respectively, with $\bar{V}_g = (C_g V_g - N - 1/2)/C_\Sigma$.

We assume that the electron-vibron coupling does not break the underlying parity symmetry of the vibronic dynamics under $X \to -X$. This follows naturally when the coupling emerges from the electron-phonon coupling *intrinsic* to the nanobeam [20] and implies that the coupling depends only on even powers of the vibronic mode coordinate X. Here, we assume that the dominant coupling is quadratic in X,

$$H_c = \frac{g}{2} X^2 \hat{n}, \tag{2}$$

with a coupling constant $g > 0$ [20]. Note that for a buckled nanobeam, this interaction generates an effectively linear coupling upon linearization about the buckled state, whose strength depends on the applied force. When there is a significant contribution to the electron-vibron coupling originating from the electrostatic dot-gate interaction, we envision a symmetric gate setup consistent with Eq. (2).

We infer characteristic scales $E_0 = g^2/\alpha$ of energy, $l_0 = \sqrt{g/\alpha}$ of length, and $\omega_0 = \sqrt{g/m}$ of frequency (or time t) by comparison of the quartic vibron potential in $H_{\rm vib}$ and the electron-vibron coupling H_c. Introducing the associated reduced variables $x = X/l_0$, $p = P/m\omega_0 l_0$, $\tau = \omega_0 t$, $v = V/E_0$, $v_g = \bar{V}_g/E_0$, and $r = R\omega_0/E_0$, we can write $H_{\rm vib} + H_c = E_0[p^2/2 + (-\epsilon + \hat{n})x^2/2 + x^4/4]$ in terms of a reduced compressional force $\epsilon = -m\omega^2/g$.

Stability analysis.—Near the instability, the vibrational dynamics becomes slow compared to the electronic tunneling dynamics. It has recently been shown [21, 22] and it is physically plausible that under these circumstances the effect of the current on the vibrational motion can be described within a NEBO approximation. The resulting Langevin description of the vibronic dynamics involves both a time-averaged and conservative current-induced force as well as fluctuating and frictional forces. We start with a stability analysis of the vibrational motion in the presence of the conservative force before we address the complete Langevin dynamics below.

Heuristically, the conservative force can be deduced by averaging the Heisenberg equation of motion $\ddot{x} = \epsilon x - x^3 - x\hat{n}$ for the vibrational coordinate over a time interval which is short compared to the time scales of the vibrational motion but long compared to the inverse of the current flowing through the nanobeam. In this way, we obtain a current-induced force $-x\langle\hat{n}\rangle_x$ where the subscript indicates that the time-averaged occupation should be computed at fixed vibron coordinate x. Assuming for definiteness that the relevant charge states involve zero and one excess electron, the dot occupation $n_0(x) = \langle\hat{n}\rangle_x$ follows from the stationary rate equation $0 = \Gamma_+(1 - n_0) - \Gamma_- n_0$. Noting that in the NEBO limit, the electron-vibron coupling enters the electronic dynamics (i.e., Γ_+ and Γ_-) via an effective x-dependent gate voltage $v_g(x) = v_g - x^2/2$, we find

$$n_0(x) = \begin{cases} 1, & x^2 < -v + 2v_g, \\ \dfrac{1}{2} + \dfrac{v_g(x)}{v}, & -v + 2v_g \leqslant x^2 \leqslant v + 2v_g, \\ 0, & x^2 > v + 2v_g, \end{cases} \tag{3}$$

with $v > 0$. Solving for the (meta)stable positions of the nanobeam by setting the effective force $f_{\rm eff}(x) = \epsilon x - x^3 - x n_0(x)$ to zero, we obtain the stability diagrams shown in Fig. 2. The most striking results of this analysis are: (i) The current flow renormalizes the critical force required for buckling towards larger values. (ii) At low biases, the buckled state can appear by a discontinuous transition.

These results can be understood most directly in terms of the potential $v_{\rm eff}(x)$ associated with $f_{\rm eff}(x)$. Focusing on the current-carrying region $\max\{0, \epsilon_-\} < x^2 < \epsilon_+$ (where $\epsilon_\pm = 2v_g \pm v$), we find

$$v_{\rm eff}(x) = \frac{1}{2}\left(-\epsilon + \frac{v + 2v_g}{2v}\right)x^2 + \frac{1}{4}\left(1 - \frac{1}{2v}\right)x^4. \tag{4}$$

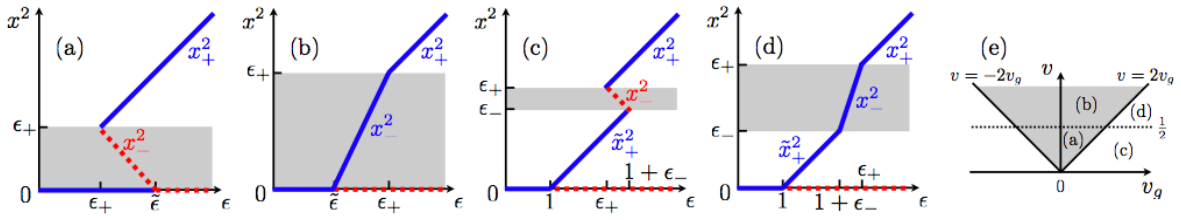

FIG. 2: (color online) (Meta)stable (solid blue lines) and unstable (dotted red lines) positions of the nanobeam as function of the scaled force ϵ applied to the beam for (a) $|v_g| < v/2$, $v < 1/2$, (b) $|v_g| < v/2$, $v > 1/2$, (c) $v_g > v/2$, $v < 1/2$ (for $\epsilon_+ > 1$; a similar plot holds for $\epsilon_+ < 1$), (d) $v_g > v/2$, $v > 1/2$. These regions of the v_g–v plane are indicated in (e). Notation: $\epsilon_\pm = 2v_g \pm v$, $\tilde{\epsilon} = 1/2 + v_g/v$, $x_+^2 = \epsilon$, $\tilde{x}_+^2 = \epsilon - 1$, and $x_-^2 = (\epsilon - \tilde{\epsilon})/(1 - 1/2v)$. The gray regions indicate conducting states.

This shows that the current-induced contribution to the harmonic part of the potential is indeed stabilizing the unbuckled state, renormalizing the critical force to $\tilde{\epsilon} = 1/2 + v_g/v$ when $\epsilon_- < 0 < \epsilon_+$ (Fig. 2a-b). Remarkably, however, the current-induced contribution to the quartic term is negative at small x^2 and thus *destabilizes* the unbuckled state. According to Eq. (4), the quartic term in the current-induced potential becomes increasingly significant as the bias voltage v decreases and we find that the overall prefactor of the quartic term becomes *negative* when $v < 1/2$. It is important to note that this does not imply a globally unstable potential since the current-induced force contributes only for small x^2. A sign reversal of the quartic term is also a familiar occurrence in the Landau theory of tricritical points which connect between second- and first-order transition lines [23]. In close analogy, the sign reversal of the quartic term in the effective potential (4) signals a discontinuous Euler instability which reverts to a continuous transition at biases $v > 1/2$ where the prefactor of the quartic term remains positive.

Specifically, when $v > 1/2$ (Fig. 2b,d), the current-induced potential renormalizes the parameters of the vibronic Hamiltonian but leaves the quartic term positive. This modifies how the position of the minimum depends on the applied force in the conducting region $\max\{0, \epsilon_-\} < x^2 < \epsilon_+$, but the Euler instability remains continuous. When $v < 1/2$, the equilibrium position at finite x becomes unstable within the entire current-carrying region. This leads to a discontinuous Euler transition when $\epsilon_- < 0 < \epsilon_+$ (Fig. 2a) and to multistability in the region $\epsilon_- < x^2 < \epsilon_+$ when $\epsilon_- > 0$ (Fig. 2c).

The gray regions with $\max\{0, \epsilon_-\} < x^2 < \epsilon_+$ in Fig. 2 indicate where the system, for a fixed x, is current carrying, with the current $I(x)$ given by $RI(x)/V = 1/4 - (v_g - x^2/2)^2/v^2$. At the level of the stability analysis, we can obtain the current by evaluating $I(x)$ at the position of the most stable minimum. Corresponding results in the v_g–v plane are shown in Fig. 3a-f for various values of the applied force ϵ.

The current blockade onset along the curved line for $v < 1/2$ is a direct consequence of the discontinuous Euler instability. In the multistable region, the current-carrying unbuckled state (the current-blocking buckled state) is the global minimum for $\epsilon < \sqrt{2v}(1/2 + v_g/v)$ [for $\epsilon > \sqrt{2v}(1/2 + v_g/v)$]. This is the novel tricritical blockade mechanism mentioned above. For $v > 1/2$ the emerging blockade is a manifestation of the Franck-Condon blockade [15, 17], caused by the induced linear electron-vibron coupling in the buckled state. Here, the current-carrying region in the v_g–v plane is given by the intersection of the Coulomb diamonds for $\hat{n} = 0$ and $\hat{n} = 1$ [17].

Langevin dynamics.—Fluctuations of the electronic occupation of the island generate a fluctuating force $\xi(\tau)$ and the delayed response of the electrons to changes in the vibronic coordinate a dissipative force $-\gamma(x)\dot{x}$, leading to Langevin dynamics of the vibronic mode described by $\ddot{x} + \gamma(x)\dot{x} = f_{\rm eff}(x) + \xi(\tau)$. To compute the quantities $\gamma(x)$ and $\xi(\tau)$, we extend the evaluation of the occupation $n(x, \tau)$ of the island beyond rate equations. Both fluctuations and vibronic dynamics are included in the Boltzmann-Langevin equation

$$\frac{dn}{dt} = \{n, H_{\rm vib}\} + \Gamma_+(1-n) - \Gamma_- n + \delta J_+ - \delta J_-. \quad (5)$$

Here, $\{.,.\}$ denotes the Poisson bracket and the Langevin sources δJ_+ and δJ_- reflect the Poisson nature of the electronic tunneling processes through the correlators $\langle \delta J_+(t)\delta J_+(t')\rangle = \Gamma_+(1-n_0)\delta(t-t')$ and $\langle \delta J_-(t)\delta J_-(t')\rangle = \Gamma_- n_0 \delta(t-t')$. Separation into equations for average and fluctuations by setting $n = \bar{n} + \delta n$ shows that the leading correction to $\bar{n}$ arises from the Poisson bracket, yielding $\bar{n} = n_0 - \frac{1}{\Gamma_+ + \Gamma_-}\dot{X}\partial_X n_0$, and that the fluctuations δn obey the correlator $\langle \delta n(t)\delta n(t')\rangle = \frac{2}{\Gamma_+ + \Gamma_-} n_0(1-n_0)\delta(t-t')$. Inserting these results into the expression for the current-induced force $-gXn$ and employing reduced units, we find $\langle \xi(\tau)\xi(\tau')\rangle = D(x)\delta(\tau - \tau')$ with diffusion and damping coefficients $D(x) = 2rx^2 n_0(1-n_0)/v$ and $\gamma(x) = -rx\partial_x n_0/v$, respectively. Finally, we can pass from the Langevin equation to the equivalent Fokker-Planck equation [21, 22] for the probability $\mathcal{P}(x, p, \tau)$ that the nanobeam is at position x and momentum p at time τ,

$$\partial_\tau \mathcal{P} = -p\partial_x \mathcal{P} - f_{\rm eff}\partial_p \mathcal{P} + \gamma \partial_p(p\mathcal{P}) + \frac{D}{2}\partial_p^2 \mathcal{P}. \quad (6)$$

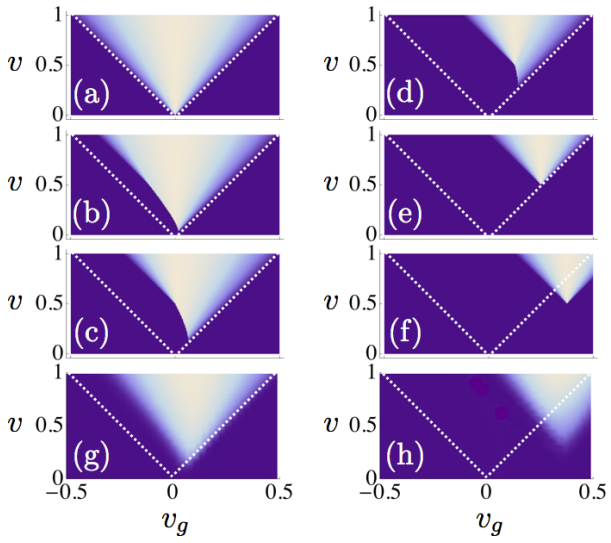

FIG. 3: (color online) Conductance $G = RI/V$ in the v_g–v plane for applied force (a) $\epsilon \leqslant 0$, (b) $\epsilon = 0.25$, (c,g) $\epsilon = 0.5$, (d) $\epsilon = 0.75$, (e) $\epsilon = 1$, (f,h) $\epsilon = 1.25$, within (a-f) stability analysis and (g-h) full Langevin dynamics ($r = \gamma_e = T = 0.01$). Color scale: $G = 0 \to 1/4$ from dark blue to white. Dotted lines delineate the Coulomb diamond for $g = 0$.

Note that the diffusion and damping coefficients are non-vanishing only in the conducting region [24].

To investigate the robustness of the stability analysis against fluctuations, we compute the current $I = \int dxdp\, \mathcal{P}_{\rm st}(x,p) I(x)$ from the stationary solution $\partial_\tau \mathcal{P}_{\rm st} = 0$ of the Fokker-Planck equation (6). Numerical results for the scaled linear conductance $G = RI/V$ are shown in Fig. 3g-h which were computed for the same parameters as the results of the stability analysis in Fig. 3c,f. We observe that the fluctuations reduce the size of the blockaded region and blur the edges of the conducting regions as the system can explore more conducting states in phase space. Nevertheless, the conclusions of the stability analysis clearly remain valid qualitatively even for the full Langevin dynamics.

Conclusion.—We have studied the Euler buckling instability in a nanoelectromechanical system as a paradigm of the interplay between a mechanical instability and current flow at the nanoscale. We have shown that the current flow modifies the nature of the buckling instability from a continuous to a tricritical transition. Likewise, the instability induces a novel tricritical current blockade at low bias. Our nonequilibrium Born-Oppenheimer approach generalizes naturally to other nanostructures such as semiconductor quantum dots or single-molecule junctions with a discrete electronic spectrum, to other types of electron-vibron coupling [25], and to additional transport characteristics such as current noise. In fact, the approach applies near any continuous mechanical instability of a nanoelectromechanical system.

Our proposed setup can be realized experimentally by clamping, e.g., a suspended carbon nanotube and applying a force to atomic precision either using a break junction or an atomic force microscope. Indeed, several recent experiments show that the electron-vibron coupling is surprisingly strong in suspended carbon nanotube quantum dots [4, 5, 16].

Acknowledgments.—We acknowledge financial support through Sfb 658 of the DFG (GW, EM, FvO) and ANR contract JCJC-036 NEMESIS (FP). FvO enjoyed the hospitality of the KITP (NSF PHY05-51164).

[1] L. D. Landau and E. M. Lifshitz, *Theory of Elasticity* (Pergamon Press, Oxford, 1970).
[2] L. Euler, in *Leonhard Euler's Elastic Curves*, translated and annotated by W. A. Oldfather, C. A. Ellis, and D. M. Brown, reprinted from ISIS, No. 58 XX(1), 1744 (Saint Catherine Press, Bruges).
[3] P. Poncharal *et al.*, Science **283**, 1513 (1999).
[4] G. A. Steele *et al.*, Science **325**, 1103 (2009).
[5] B. Lassagne *et al.*, Science **325**, 1107 (2009).
[6] M. R. Falvo *et al.*, Nature **389**, 582 (1997).
[7] S. M. Carr and M. N. Wybourne, Appl. Phys. Lett. **82**, 709 (2003).
[8] W. Bao *et al.*, Nature Nanotechnology DOI: 10.1038/nnano.2009.191 (2009).
[9] J. C. Meyer *et al.*, Nature **446**, 60 (2007).
[10] S. M. Carr, W. E. Lawrence, and M. N. Wybourne, Phys. Rev. B **64**, 220101 (2001).
[11] P. Werner and W. Zwerger, Europhys. Lett. **65**, 158 (2004).
[12] V. Peano and M. Thorwart, New J. Phys. **8**, 21 (2006).
[13] S. Savel'ev, X. Hu, and F. Nori, New J. Phys. **8**, 105 (2006).
[14] H. G. Craig, Science **290**, 1532 (2000); M. L. Roukes, Phys. World **14**, 25 (2001).
[15] J. Koch and F. von Oppen, Phys. Rev. Lett. **94**, 206804 (2005).
[16] R. Leturcq *et al.*, Nature Physics **5**, 327 (2009).
[17] F. Pistolesi and S. Labarthe, Phys. Rev. B **76**, 165317 (2007).
[18] The rotation of the plane of the buckled nanobeam is assumed massive due to clamped boundary conditions.
[19] See, e.g., Chap. 3 in T. Dittrich *et al.*, *Quantum Transport and Dissipation* (Wiley-VCH, Weinheim, 1998).
[20] E. Mariani and F. von Oppen, arXiv:0904.4653.
[21] Ya. M. Blanter, O. Usmani, and Yu. V. Nazarov, Phys. Rev. Lett. **93**, 136802 (2004); *ibid.* **94**, 049904(E) (2005).
[22] D. Mozyrsky, M. B. Hastings, and I. Martin, Phys. Rev. B **73**, 035104 (2006).
[23] See, e.g., P. M. Chaikin and T. C. Lubensky, *Principles of Condensed Matter Physics* (Cambridge University Press, Cambridge, 1995).
[24] In some cases, a stable numerical solution of Eq. (6) requires a small extrinsic damping γ_e and temperature T.
[25] E.g., a small symmetry-breaking coupling linear in X leads to a tricritical point in an external field while a purely linear coupling to a 2nd order transition in a field, G. Weick *et al.*, unpublished.